THE JOURNAL OF PHYSICAL CHEMISTRY Letters

Letter

pubs.acs.org/JPCL

The Use of Mn(II) Bound to His-tags as Genetically Encodable Spin-Label for Nanometric Distance Determination in Proteins

H. Y. Vincent Ching,[†] Florencia C. Mascali,[‡] Hélène C. Bertrand,[§,¶,⊥] Eduardo M. Bruch,[†] Paul Demay-Drouhard,[§,¶,⊥] Rodolfo M. Rasia,[‡] Clotilde Policar,[§,¶,⊥] Leandro C. Tabares,*[,†] and Sun Un*[,†]

[†]Institute for Integrative Biology of the Cell (I2BC), Department of Biochemistry, Biophysics and Structural Biology, Université Paris-Saclay, CEA, CNRS UMR 9198, F-91191 Gif-sur-Yvette, France

[‡]Instituto de Biología Molecular y Celular de Rosario; Área Biofísica, Facultad de Ciencias Bioquímicas y Farmacéuticas, Universidad Nacional de Rosario, 2000 Rosario, Argentina

[§]Ecole Normale Supérieure-PSL Research University, Département de Chimie, Sorbonne Universités - UPMC Univ Paris 06, CNRS UMR 7203 LBM, F-75005 Paris, France

[¶]CNRS, UMR 7203, Laboratoire des Biomolécules, F-75005 Paris, France

[⊥]Sorbonne Universités, UPMC Univ Paris 06, UMR 7203, Laboratoire des Biomolécules, F-75005 Paris, France

Supporting Information

ABSTRACT: A genetically encodable paramagnetic spin-label capable of self-assembly from naturally available components would offer a means for studying the in-cell structure and interactions of a protein by electron paramagnetic resonance (EPR). Here, we demonstrate pulse electron−electron double resonance (DEER) measurements on spin-labels consisting of Mn(II) ions coordinated to a sequence of histidines, so-called His-tags, that are ubiquitously added by genetic engineering to facilitate protein purification. Although the affinity of His-tags for Mn(II) was low (800 μM), Mn(II)-bound His-tags yielded readily detectable DEER time traces even at concentrations expected in cells. We were able to determine accurately the distance between two His-tag Mn(II) spin-labels at the ends of a rigid helical polyproline peptide of known structure, as well as at the ends of a completely cell-synthesized 3-helix bundle. This approach not only greatly simplifies the labeling procedure but also represents a first step towards using self-assembling metal spin-labels for in-cell distance measurements.

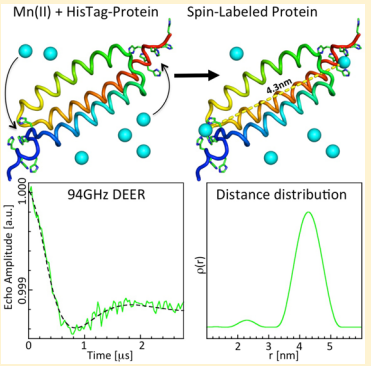

There are few *in situ* techniques that are able to probe the structures of proteins and their interactions in cells. This is important because cellular environments are complex and can significantly differ from test tube conditions. Pulse electron−electron double resonance (PELDOR or DEER)[1,2] is able to measure distances on a nanometer scale, and it has become a proven method for studying structures in biological systems.[3−5] One of its great advantages is that it can be applied to systems in a wide variety of environments, even inside cells.[6−11] A very recent elegant application has been the conformational study of α-synuclein introduced into mammalian cells by electroporation.[11] Conventional nitroxide-based spin-labels used in DEER measurements have limited stability in the reducing cytosolic environment.[12] Metal-based spin-labels are more appealing.[9−11] To date, such labels have involved a redox stable paramagnetic metal ion encapsulated inside a well-defined ligand sphere that has a high binding affinity for the metal.[9,10,13−18] Nearly all ligand systems used are synthetic and, like nitroxide, require a linking group. There have been two exceptions: the use of Cu(II) to bind to two nearby histidines and exogenous iminodiacetate[19] and Gd(III) bound to a Lanthanide Binding Tag,[20] an amino-acid sequence which has a high affinity for lanthanides and that can be genetically encoded into a protein. Here we examine a different approach, the use of Mn(II) bound to His-tags as spin-labels. His-tags, typically a sequence of six histidines placed at the ends of proteins, provide a simple and effective means of protein purification based on Ni^{2+}-affinity chromatography and, as such, have become a routine tool in protein chemistry and molecular biology.[21,22] His-tags have already been used once in DEER measurements as anchoring sites for a trinuclear Ni^{2+} complex carrying a nitroxide spin-label.[23] This allowed specific labeling of a His-tagged protein even in a complicated cellular lysate mixture, which in principle could also be used for in-cell applications. Unlike nickel and copper, Mn(II) is not toxic and is also both redox stable and most importantly endogenous to cells. Hence, the combination of Mn(II) and His-tags is appealing for use as spin-labels. The affinity of His-tags for Mn(II) has not been studied in detail, but it is likely to be low. As will be seen, this does not significantly impair the use of

Received: February 17, 2016
Accepted: March 3, 2016

DOI: 10.1021/acs.jpclett.6b00362
J. Phys. Chem. Lett. 2016, 7, 1072−1076

Mn(II) bound to His-tags as spin-labels for DEER distance measurements. This combination offers the possibility of spin-labels that are self-assembled from naturally available components within cells with which in-cell DEER measurements can be made. We will show that this approach is feasible and describe DEER measurements on Mn(II) bound to 3- and 6-histidine His-tags attached to the ends of a nine-proline synthetic peptide that forms a rigid helical structure, which we designate as $H_3P_9H_3$ and $H_6P_9H_6$, and a 6-histidine His-tag genetically encoded into a three helix bundle (3Hx)[24] which was overexpressed and isolated from cells (see Supporting Information for sequence and further details), which we designate $MGDH_63HxH_6$ (Figure 1).

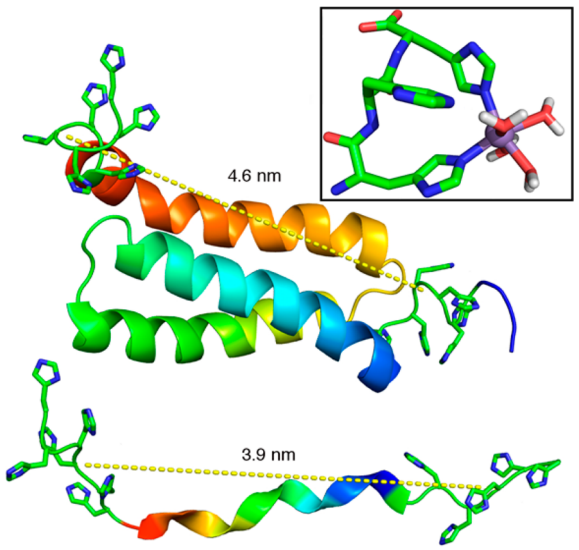

Figure 1. Structures of $MGDH_63HxH_6$ (top panel) and $H_6P_9H_6$ (bottom panel). The central peptide portions are shown as ribbons, and the 6-histidine tags are shown as sticks. The distances were obtained from molecular dynamics calculations (see text and Supporting Information for details). The inset shows a DFT (BLY3P/6-31+G(p,d)) derived structure of a Mn(II) ligated to a 3-histidine peptide in water consistent with data from the EPR measurements.

Figure 2 summarizes the results from 94 GHz Mn(II) EPR, ^{55}Mn electron nuclear double resonance (ENDOR), and electron−electron double resonance (ELDOR)-NMR measurements on a solution of 600 μM Mn(II) and 300 μM $H_6P_9H_6$, concentrations that are comparable to those found in cells.[25] The strong single- and double-quantum ^{14}N ELDOR-NMR resonances (Figure 2C) were very similar to those of Mn(II) imidazole complexes.[26] The ^{14}N hyperfine coupling, obtained from splitting of the double-quantum resonance, was 2.7 MHz. The ^{55}Mn ENDOR spectrum of the solution (Figure 2B) exhibited a partially resolved resonance arising from two species with different ^{55}Mn hyperfine couplings. For Mn(II) complexes involving imidazole ligands, there is a linear relationship between the number of imidazole ligands and the ^{55}Mn hyperfine coupling.[26] The ENDOR spectrum was reproduced by adding the spectrum of $[Mn(H_2O)_6]^{2+}$ and $[Mn(imidazole)_2(H_2O)_4]^{2+}$ in about a 2:1 ratio. In a similar manner, it was possible to determine that the zero-field parameters of the nitrogen bound centers were D = −980 MHz and E = 327 MHz (see Supporting Information). A structure derived from DFT calculations (see Supporting Information for

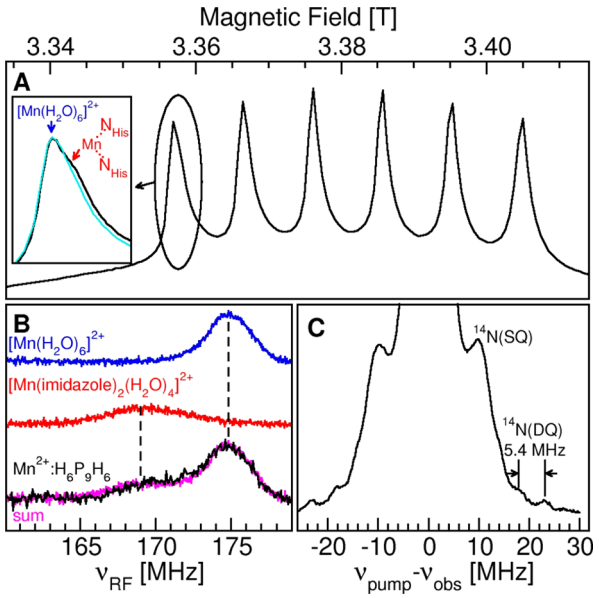

Figure 2. EPR spectra (94 GHz) of 600 μM Mn(II) with 300 μM $H_6P_9H_6$ (black). (A) The 4.5 K field-swept spin−echo spectrum. The inset shows an expanded view of the first hyperfine line compared to that of the comparable solution of Mn(II) and $MGDH_63HxH_6$ (cyan). The inset labels and arrows show the positions of the contribution from $[Mn(H_2O)_6]^{2+}$ (blue) and Mn(II) centers bound to two histidines (red). (B) The 6 K ^{55}Mn Davies ENDOR spectrum and the sum (magenta) of the spectra of $[Mn(H_2O)_6]^{2+}$ (blue) and $[Mn(imidazole)_2(H_2O)_4]^{2+}$ (red) in a 2:1 ratio. (C) The 6 K ELDOR-NMR spectrum showing the ^{14}N single- and double-quantum (ν^{14}_N = 10 MHz) resonances.

further details) consistent with these ENDOR and ELDOR-NMR measurements is shown in Figure 1 (inset). The calculated isotropic ^{14}N hyperfine coupling constant for the two ligating nitrogens was 2.4 MHz with anisotropy tensor of [−1.8, −1.9, 3.6] MHz. Modeling studies showed that the ligand sphere of a Mn(II) bound to two histidines with an intervening nonligating ligand residue could easily form an octahedral geometry complex, whereas those involving adjacent histidines were strained. These results showed that there were significant concentrations of the Mn(II):$H_6P_9H_6$ and Mn(II):$H_6P_9H_6$:Mn(II) complexes present that had the Mn(II) ions bound to two imidazole side groups of histidine residues. From the data, the apparent His-tag K_d for Mn(II) in $H_6P_9H_6$ was crudely estimated to be 800 μM, with Mn(II):$H_6P_9H_6$:Mn(II) constituting about 6% of the total Mn(II) (see Supporting Information).

As shown in Figure 3, these doubly Mn(II) labeled molecules gave rise to a readily detectable DEER modulation. The background of the DEER time trace could be adequately modeled with a linear function (Figure 3A,B); however, a combination of linear and stretched exponential functions yielded more ideal frequency-domain Pake patterns. Measurements on a control sample containing 600 μM Mn(II) and 600 μM P_9H_6 peptide yielded a flat DEER response after background correction. The modulation depth arising from Mn(II):$H_6P_9H_6$:Mn(II), as expected, was small, about 0.4% compared to high-affinity Mn(II) spin-labels that had modulation depths of 1−2%.[15,16] Tikhonov analysis (Figure 3C) showed the most probable Mn(II)−Mn(II) distance was 4.0(2.2) nm (where the number in parentheses specifies the width of the distribution at half height). This was nearly the

DOI: 10.1021/acs.jpclett.6b00362
J. Phys. Chem. Lett. 2016, 7, 1072−1076

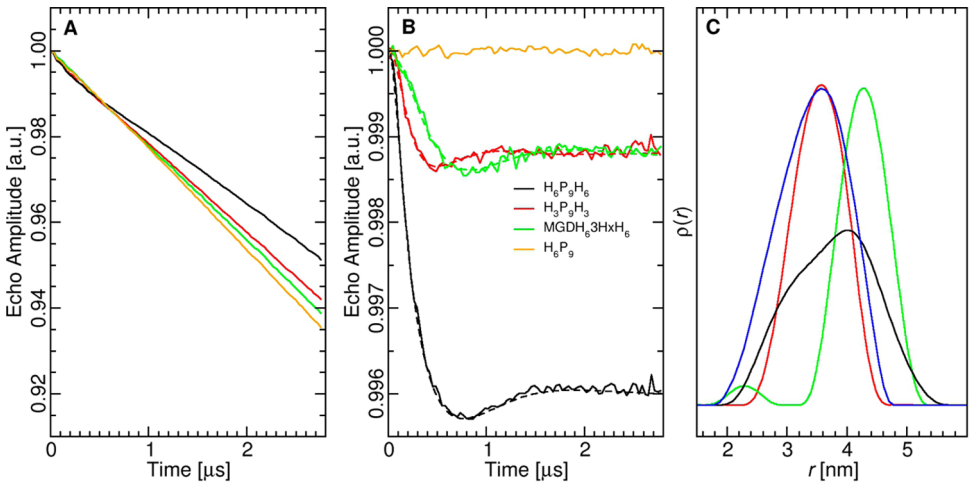

Figure 3. DEER measurements on a solution containing 600 μM Mn(II) and 300 μM $H_6P_9H_6$ (black), $H_3P_9H_3$ (red), $MGDH_63HxH_6$ (green), and 600 μM Mn(II) and 600 μM P_9H_6 (orange): (A) normalized DEER time traces; (B) with background removed (solid line) along with fits based on the Tikhonov analysis (dashed lines) for the corresponding distance distributions shown in panel C. The blue trace shows the previously measured distance distribution profile for MnDOTA*m*CP$_9$C*m*MnDOTA[16] (see text for details). Typical measurement times were 48−60 h.

same as the average distance between the centers of gravities of the six nonprotonated nitrogens of each His-tag of 3.9(1.0) nm determined from molecular dynamics simulation of $H_6P_9H_6$, that is, the peptide without Mn(II).

Measurements on Mn(II):$H_3P_9H_3$:Mn(II) revealed further details about binding and the distance distribution inherent to the Mn(II):His-tag spin-label. The modulation depth of the Mn(II):$H_3P_9H_3$:Mn(II) was slightly larger than 0.1% (Figure 3B). One simple interpretation is that the factor of 4 difference with respect to Mn(II):$H_6P_9H_6$:Mn(II) reflects the smaller number of $^{-H}_{-H}\!\!>\!Mn^{2+}\!<\!^{-H}_{-H}$ binding motifs that are possible. Consistent with this, the ^{55}Mn ENDOR intensity corresponding to the two histidine binding sites was lower. Tikhonov analysis yielded a distance of 3.6(1.1) nm, shorter and substantially narrower in distribution than for the six-histidine tag (Figure 3C). This was consistent with the molecular dynamics-derived average $H_3P_9H_3$ His-tags distance of 3.4(0.6) nm.

To examine how generalizable His-tags were, we genetically encoded a 3-helix bundle[24] with two His-tags at both ends (Figure 1) and overexpressed and isolated it from *Escherichia coli*. The EPR spectrum of a frozen solution of 300 μM $MGDH_63HxH_6$ and 600 μM Mn(II) was nearly identical to that of one containing $H_6P_9H_6$ (Figure 2A, inset). The DEER time trace of Mn(II):$MGDH_63HxH_6$:Mn(II) was similar to those of Mn(II):$H_3P_9H_3$:Mn(II) with a modulation depth of 0.1%, but with a slower initial decay indicative of longer Mn(II)−Mn(II) distances. Tikhonov analysis yielded a distance of 4.3(1.0) nm (see Figure S3 for other details). Molecular dynamics simulations showed that the average calculated His-tag distance in $MGDH_63HxH_6$ was 4.6(0.4) nm, determined from the structures predicted by the QUARK[27] and ROBETTA[28,29] de novo protein structure prediction algorithms. The smaller modulation depth compared to Mn(II):$H_6P_9H_6$:Mn(II) suggested that not all of the His-tag histidines in the 3-helix construct were involved in Mn(II) binding. The predicted structure revealed that two of the histidines at both ends were integrated into the helical structure (Figure 1), most likely making them less available for binding to Mn(II); consequently, the six-histidine tags probably acted as if they were three-histidine tags. The lower intensity of the region of the EPR spectrum corresponding to Mn(II) bound to two histidines in Figure 2A (inset) was consistent with a smaller number of $^{-H}_{-H}\!\!>\!Mn^{2+}\!<\!^{-H}_{-H}$ type binding sites (Figure 1 inset). The 3-helix bundle His-tags were also more conformationally constrained than in $H_6P_9H_6$. The comparatively small distance distribution of Mn(II):$MGDH_63HxH_6$:Mn(II) was consistent with this. For example, due to steric interactions, the labels could not fold-back toward each other. In general, His-tags, irrespective of length and environment, will likely have multiple Mn(II) binding configurations which will contribute to the DEER distance distributions. However, the distance distribution of Mn(II):$MGDH_63HxH_6$:Mn(II), along with the even smaller distribution of Mn(II):$H_3P_9H_3$:Mn(II), were both smaller than those of MnDOTA*m*CP$_n$C*m*MnDOTA (where *m* denotes the maleimide linker).[16] For example, the distribution for MnDOTA*m*CP$_9$C*m*MnDOTA was 1.5 nm at a Mn−Mn distance comparable to those of Mn(II):$H_3P_9H_3$:Mn(II) and Mn(II):$H_6P_9H_6$:Mn(II) (Figure 3C).[16] Aside from the conformational flexibility of the maleimide−cysteine linkage, the broad distributions of the MnDOTA*m*CP$_n$C*m*MnDOTA complexes were also ascribed to pseudosecular dipolar contributions arising from close energetic similarities of the spin-labels owing to their small zero-field interactions.[16]

The His-tags regardless of their lengths were likely to have smaller pseudosecular dipolar contribution than MnDOTA in part because of their larger zero-field interaction (see Supporting Information).[16] This would result in a smaller apparent distance distribution because such contributions are not explicitly accounted for by the Tikhonov kernel and hence appear in the distance profiles as additional components.[16] This meant that in addition to the ability to genetically encode His-tags directly onto proteins and overexpression of such proteins in cells, Mn(II) His-tag spin-labels also have appealing spectroscopic advantages. These could further be enhanced using techniques such as a frequency-swept DEER pump pulse,[30] which has been shown to increase modulation-depth, and other techniques such as relaxation-induced dipolar modulation enhancement,[31,32] an alternative to DEER based on relaxation effects. These approaches are being examined.

DOI: 10.1021/acs.jpclett.6b00362
J. Phys. Chem. Lett. 2016, 7, 1072−1076

His-tags are likely to work best at exposed termini of proteins making them more appropriate for problems involving quaternary structure and protein−protein interactions. Although we were able to obtain reliable results even under in-cell concentration[25] conditions, it is likely that His-tags can be modified to improve their Mn(II) binding affinity, for example by inserting a carboxylic acid residue between the two ligating histidines (Figure 1, inset). The important point of our approach is that the target protein(s) can be produced biosynthetically with His-tags genetically encoded and spin-labeled with endogenous Mn(II) all within the cell, providing a potential means for making in-cell structural measurements. To date there have been just a few reports of in-cell DEER measurements, and all have used microinjection or electroporation to introduce the labeled protein into the cell.[6−11,33] The use of unnatural amino-acids (UAA) is a more elegant approach that is being explored.[14,33] It has been shown that UAA can be used to biosynthetically incorporate a nitroxide spin-label into a protein[33] and to introduce specific positions at which *in situ* "click" chemistry can be used to attach spin-labels.[14] They could also be used to incorporate metal−ligands.[34] However, the use of UAA requires much more extensive and complex molecular biological machinery that is only now being developed. By comparison, genetically encoded His-tags are ubiquitous and may in certain cases provide an elegantly simple means for producing a Mn(II) spin-label that can be used to make structural studies. A number of different applications are being explored.

■ ASSOCIATED CONTENT

Supporting Information

The Supporting Information is available free of charge on the ACS Publications website at DOI: 10.1021/acs.jpclett.6b00362.

Mn(II):$H_6P_9H_6$:Mn(II) apparent K_d and zero-field splitting determination, details of the N- and C-termini $MGDH_63HxH_6$ structure, decomposition of the Tikhonov distance distribution profile for Mn(II):$MGDH_63HxH_6$:Mn(II), and experimental and computational procedures (PDF)

■ AUTHOR INFORMATION

Corresponding Authors

*S.U.: Bat 532 Pce 210, F-91191 Gif-sur-Yvette, France; phone, +33-169082842; e-mail, sun.un@cea.fr.

*L.T.: Bat 532 Pce 215, F-91191 Gif-sur-Yvette, France; phone, +33-169087579; e-mail, leandro.tabares@cea.fr.

Notes

The authors declare no competing financial interest.

■ ACKNOWLEDGMENTS

We thank F. Leach for useful comments. This work was partially financed by the ANR (2011-INTB-1010-01), the French Infrastructure for Integrated Structural Biology (FRISBI, ANR-10-INSB-05-01), the ECOS/Sud program (A14B02), and ANPCyT from Argentina (PICT-2012-1702). The spectrometer was funded by the Région Ile-de-France "Sesame" program, the CEA, and CNRS.

■ REFERENCES

(1) Milov, A. D.; Ponomarev, A. B.; Tsvetkov, Y. D. Electron-Electron Double Resonance in Electron Spin Echo: Model Biradical Systems and the Sensitized Photolysis of Decalin. *Chem. Phys. Lett.* **1984**, *110*, 67−72.

(2) Martin, R. E.; Pannier, M.; Diederich, F.; Gramlich, V.; Hubrich, M.; Spiess, H. W. Determination of End-to-End Distances in a Series of TEMPO Diradicals of up to 2.8 Nm Length with a New Four-Pulse Double Electron Electron Resonance Experiment. *Angew. Chem., Int. Ed.* **1998**, *37*, 2833−2837.

(3) Schiemann, O.; Prisner, T. F. Long-Range Distance Determinations in Biomacromolecules by EPR Spectroscopy. *Q. Rev. Biophys.* **2007**, *40*, 1−53.

(4) Tsvetkov, Y. D.; Milov, A. D.; Maryasov, A. G. Pulsed Electron-Electron Double Resonance (PELDOR) as EPR Spectroscopy in Nanometre Range. *Russ. Chem. Rev.* **2008**, *77*, 487−520.

(5) Jeschke, G. DEER Distance Measurements on Proteins. *Annu. Rev. Phys. Chem.* **2012**, *63*, 419−446.

(6) Azarkh, M.; Okle, O.; Singh, V.; Seemann, I. T.; Hartig, J. S.; Dietrich, D. R.; Drescher, M. Long-Range Distance Determination in a DNA Model System inside Xenopus Laevis Oocytes by In-Cell Spin-Label EPR. *ChemBioChem* **2011**, *12*, 1992−1995.

(7) Igarashi, R.; Sakai, T.; Hara, H.; Tenno, T.; Tanaka, T.; Tochio, H.; Shirakawa, M. Distance Determination in Proteins inside Xenopus Laevis Oocytes by Double Electron−Electron Resonance Experiments. *J. Am. Chem. Soc.* **2010**, *132*, 8228−8229.

(8) Krstić, I.; Hänsel, R.; Romainczyk, O.; Engels, J. W.; Dötsch, V.; Prisner, T. F. Long-Range Distance Measurements on Nucleic Acids in Cells by Pulsed EPR Spectroscopy. *Angew. Chem., Int. Ed.* **2011**, *50*, 5070−5074.

(9) Qi, M.; Groß, A.; Jeschke, G.; Godt, A.; Drescher, M. Gd(III)-PyMTA Label Is Suitable for In-Cell EPR. *J. Am. Chem. Soc.* **2014**, *136*, 15366−15378.

(10) Martorana, A.; Bellapadrona, G.; Feintuch, A.; Di Gregorio, E.; Aime, S.; Goldfarb, D. Probing Protein Conformation in Cells by EPR Distance Measurements Using Gd^{3+} Spin Labeling. *J. Am. Chem. Soc.* **2014**, *136*, 13458−13465.

(11) Theillet, F.-X.; Binolfi, A.; Bekei, B.; Martorana, A.; Rose, H. M.; Stuiver, M.; Verzini, S.; Lorenz, D.; van Rossum, M.; Goldfarb, D.; et al. Structural Disorder of Monomeric α-Synuclein Persists in Mammalian Cells. *Nature* **2016**, *530*, 45−50.

(12) Jagtap, A. P.; Krstic, I.; Kunjir, N. C.; Hänsel, R.; Prisner, T. F.; Sigurdsson, S. T. Sterically Shielded Spin Labels for in-Cell EPR Spectroscopy: Analysis of Stability in Reducing Environment. *Free Radical Res.* **2015**, *49*, 78−85.

(13) Matalon, E.; Huber, T.; Hagelueken, G.; Graham, B.; Frydman, V.; Feintuch, A.; Otting, G.; Goldfarb, D. Gadolinium(III) Spin Labels for High-Sensitivity Distance Measurements in Transmembrane Helices. *Angew. Chem., Int. Ed.* **2013**, *52*, 11831−11834.

(14) Abdelkader, E. H.; Feintuch, A.; Yao, X.; Adams, L. a.; Aurelio, L.; Graham, B.; Goldfarb, D.; Otting, G. Protein Conformation by EPR Spectroscopy Using Gadolinium Tags Clicked to Genetically Encoded P-Azido-L-Phenylalanine. *Chem. Commun.* **2015**, *51*, 15898−15901.

(15) Banerjee, D.; Yagi, H.; Huber, T.; Otting, G.; Goldfarb, D. Nanometer-Range Distance Measurement in a Protein Using Mn^{2+} Tags. *J. Phys. Chem. Lett.* **2012**, *3*, 157−160.

(16) Vincent Ching, H. Y.; Demay-Drouhard, P.; Bertrand, H. C.; Policar, C.; Tabares, L. C.; Un, S. Nanometric Distance Measurements between Mn(II)DOTA Centers. *Phys. Chem. Chem. Phys.* **2015**, *17*, 23368−23377.

(17) Martorana, A.; Yang, Y.; Zhao, Y.; Li, Q.; Su, X.-C.; Goldfarb, D. Mn(II) Tags for DEER Distance Measurements in Proteins via C−S Attachment. *Dalt. Trans.* **2015**, *44*, 20812−20816.

(18) Cunningham, T. F.; Shannon, M. D.; Putterman, M. R.; Arachchige, R. J.; Sengupta, I.; Gao, M.; Jaroniec, C. P.; Saxena, S. Cysteine-Specific Cu^{2+} Chelating Tags Used as Paramagnetic Probes in Double Electron Electron Resonance. *J. Phys. Chem. B* **2015**, *119*, 2839−2843.

(19) Cunningham, T. F.; Putterman, M. R.; Desai, A.; Horne, W. S.; Saxena, S. The Double-Histidine Cu^{2+} -Binding Motif: A Highly Rigid,

DOI: 10.1021/acs.jpclett.6b00362
J. Phys. Chem. Lett. 2016, 7, 1072−1076

Site-Specific Spin Probe for Electron Spin Resonance Distance Measurements. *Angew. Chem., Int. Ed.* **2015**, *54*, 6330−6334.
(20) Barthelmes, D.; Gränz, M.; Barthelmes, K.; Allen, K. N.; Imperiali, B.; Prisner, T.; Schwalbe, H. Encoded Loop-Lanthanide-Binding Tags for Long-Range Distance Measurements in Proteins by NMR and EPR Spectroscopy. *J. Biomol. NMR* **2015**, *63*, 275−282.
(21) Bornhorst, J. A.; Falke, J. J. Purification of Proteins Using Polyhistidine Affinity Tags. *Methods Enzymol.* **2000**, *326*, 245−254.
(22) Block, H.; Maertens, B.; Spriestersbach, A.; Brinker, N.; Kubicek, J.; Fabis, R.; Labahn, J.; Schäfer, F. Immobilized-Metal Affinity Chromatography (IMAC). *Methods Enzymol.* **2009**, *463*, 439−473.
(23) Baldauf, C.; Schulze, K.; Lueders, P.; Bordignon, E.; Tampé, R. In-Situ Spin Labeling of His-Tagged Proteins: Distance Measurements under In-Cell Conditions. *Chem. - Eur. J.* **2013**, *19*, 13714−13719.
(24) Huang, P.-S.; Oberdorfer, G.; Xu, C.; Pei, X. Y.; Nannenga, B. L.; Rogers, J. M.; DiMaio, F.; Gonen, T.; Luisi, B.; Baker, D. High Thermodynamic Stability of Parametrically Designed Helical Bundles. *Science* **2014**, *346*, 481−485.
(25) Bruch, E. M.; de Groot, A.; Un, S.; Tabares, L. C. The Effect of Gamma-Ray Irradiation on the Mn(II) Speciation in *Deinococcus radiodurans* and the Potential Role of Mn(II)-Orthophosphates. *Metallomics* **2015**, *7*, 908−916.
(26) Un, S. Structure and Nature of manganese(II) Imidazole Complexes in Frozen Aqueous Solutions. *Inorg. Chem.* **2013**, *52*, 3803−3813.
(27) Xu, D.; Zhang, Y. *Ab Initio* Protein Structure Assembly Using Continuous Structure Fragments and Optimized Knowledge-Based Force Field. *Proteins: Struct., Funct., Genet.* **2012**, *80*, 1715−1735.
(28) Raman, S.; Vernon, R.; Thompson, J.; Tyka, M.; Sadreyev, R.; Pei, J.; Kim, D.; Kellogg, E.; DiMaio, F.; Lange, O.; et al. Structure Prediction for CASP8 with All-Atom Refinement Using Rosetta. *Proteins: Struct., Funct., Genet.* **2009**, *77*, 89−99.
(29) Kim, D. E.; Chivian, D.; Baker, D. Protein Structure Prediction and Analysis Using the Robetta Server. *Nucleic Acids Res.* **2004**, *32*, W526−W531.
(30) Doll, A.; Qi, M.; Wili, N.; Pribitzer, S.; Godt, A.; Jeschke, G. Gd(III)-Gd(III) Distance Measurements with Chirp Pump Pulses. *J. Magn. Reson.* **2015**, *259*, 153−162.
(31) Razzaghi, S.; Qi, M.; Nalepa, A. I.; Godt, A.; Jeschke, G.; Savitsky, A.; Yulikov, M. RIDME Spectroscopy with Gd(III) Centers. *J. Phys. Chem. Lett.* **2014**, *5*, 3970−3975.
(32) Milikisyants, S.; Scarpelli, F.; Finiguerra, M. G.; Ubbink, M.; Huber, M. A Pulsed EPR Method to Determine Distances between Paramagnetic Centers with Strong Spectral Anisotropy and Radicals: The Dead-Time Free RIDME Sequence. *J. Magn. Reson.* **2009**, *201*, 48−56.
(33) Schmidt, M. J.; Borbas, J.; Drescher, M.; Summerer, D. A Genetically Encoded Spin Label for Electron Paramagnetic Resonance Distance Measurements. *J. Am. Chem. Soc.* **2014**, *136*, 1238−1241.
(34) Liu, C. C.; Schultz, P. G. Adding New Chemistries to the Genetic Code. *Annu. Rev. Biochem.* **2010**, *79*, 413−444.

DOI: 10.1021/acs.jpclett.6b00362
J. Phys. Chem. Lett. 2016, 7, 1072−1076